J.Atmos. Sol. -Terr. Phys., vol. 157-158, 35-41, 2017,http://dx.doi.org/10.1016/j.jastp.2017.03.016

Unexpected East-West effect in mesopause region SABER temperatures over El Leoncito

Esteban R. Reisin* and Jürgen Scheer

Instituto de Astronomía y Física del Espacio, CONICET - Universidad de Buenos Aires. Buenos Aires, Argentina.

* Corresponding author: Esteban R. Reisin, Instituto de Astronomía y Física del Espacio, Ciudad Universitaria, C.C. 67 Suc. 28, 1428 Buenos Aires, Argentina (ereisin@iafe.uba.ar).

Abstract

We find that mesopause region temperatures determined by the SABER instrument on the TIMED satellite during nocturnal overpasses at El Leoncito (31.8°S, 69.3°W) are several kelvins higher when SABER observes from the East than when it observes from the West. We distinguish between altitudes corresponding to the nominal emission heights of the OH and O_2 airglow layers. The East-West temperature differences of 4.5K obtained for OH-equivalent height, and of 3.5K for O_2-equivalent height are surprising, because an effect of the South Atlantic Anomaly on SABER temperature is unexpected. However, the ground-based data obtained with our airglow spectrometer at El Leoncito show that such a SABER artifact can be ruled out. Rather, the phenomenon is explained as a consequence of the temporal sampling of the nocturnal variation, which is mostly due to the semidiurnal tide. The monthly mean tide is strongest from April to September with a mean amplitude of 6.9K for OH, and of 10.5K for O_2 rotational temperature, but the contribution to the East-West effect varies strongly from month to month because of differences in the temporal sampling. This mechanism should be active at other sites, as well.

Keywords: Airglow; Mesopause region; Rotational temperature; SABER temperature; Semidiurnal tide; South Atlantic Anomaly

1. Introduction

As has often been emphasized, ground-based and satellite-based observations of the upper atmosphere are complementary. Satellite data may provide global coverage while local time coverage at a given place is limited. In case of a sun-synchronous orbit, data for only two fixed local times are obtained at a given site. On the other hand, ground-based data may provide near continuous local time coverage but of course, only near a given geographical site. For this reason, the combination of ground-based and satellite data is useful to overcome these limitations. Such a combination has widely been used in the literature and even for the specific topic of mesopause region temperatures there have been several recent geophysical studies, e. g., Xu et al. (2006), French and Mulligan (2010), Yuan et al. (2010), Reisin et al. (2014). In the same context, also data quality assessments may be cited, e. g., von Savigny et al. (2004), Siskind et al. (2005), Oberheide et al. (2006), Scheer et al. (2006), López-González et al. (2007), Kumar et al., (2008), Mulligan and Lowe (2008), Remsberg et al. (2008), Smith et al. (2010), Scheer and Reisin (2013), Liu et al. (2015).

Among the papers mentioned, von Savigny et al. (2004), Siskind et al. (2005), Oberheide et al. (2006), Scheer et al. (2006), Xu et al. (2006), López-Gónzalez et al. (2007), French and Mulligan (2010), Smith et al. (2010), and Liu et al. (2015) report mesopause region temperature intercomparisons, and are therefore most relevant to the context of the present paper. Most comparisons (7 of 9) are with the SABER (Sounding of the Atmosphere using Broadband Emission Radiometry) instrument (Russell III et al., 1999) on the TIMED (Thermosphere Ionosphere Mesosphere Energetics and Dynamics) satellite. The other two instruments are SCIAMACHY and CRISTA used by von Savigny et al. (2004) and Scheer et al., (2006), respectively.

All of these satellite instruments operate in limb scan mode, which implies the need for conversion from the observed signal variations to vertical profiles. The volume element of interest in the upper atmosphere (the tangent point, TP) is at great distance from the satellite (depending on the heights of the satellite and the TP). In comparison with ground-based observations, exactly the same volume element is nearly never involved, so that miss distance and miss time effects have to be dealt with. Also, satellite overpass data inevitably only represent a small fraction of the available ground-based data because overpasses typically do not occur more than twice per 24 hours. Meaningful intercomparisons therefore typically require considerable averaging.

While averaging can be expected to improve statistics, it does not in itself remove any trace of possible bias. For example, such a bias can be produced by the satellite position with respect to the TP. Auroral contamination is likely to depend on observation geometry, and so does particle precipitation in the region of the South Atlantic Anomaly. Particle precipitation may cause effects as dramatic as memory errors in satellite electronics, more moderate reduction of data quality as in the spectra of the TIDI instrument on the TIMED satellite (Niciejewski et al., 2006), or small drifts as in the DORIS oscillator frequency on the SPOT-5 satellite (Štěpánek et al., 2013).

In the present paper, we use our own dataset of mesopause region temperatures obtained with the ground-based spectrometer at the Argentine midlatitude site El Leoncito in combination with SABER temperatures at the same altitude. We find a pronounced perspective effect in the satellite data depending on viewing direction towards El Leoncito, from the Atlantic or the Pacific Ocean, which mimics a South Atlantic Anomaly effect. Comparison with ground-based data is vital for leading to the correct interpretation of this surprising East-West asymmetry.

2. Ground-based and SABER data

The ground-based data from El Leoncito (LEO; 31.8°S, 69.3°W) are obtained with the Argentine Airglow Spectrometer (AAS), a tilting filter spectrometer for the nocturnal emissions of the OH(6-2) and O_2b(0-1) airglow bands (Scheer, 1987; Scheer and Reisin, 2001). The OH and O_2 band intensities and rotational temperatures are obtained with a time resolution of about 80 seconds. These temperatures correspond to the nominal centroid heights of the OH and O_2 layers, at 87 km and 95 km, respectively. We here use the temperatures from 2006 to 2014, excluding the previous data to avoid the issue of systematic offset discussed in Scheer and Reisin (2013). Data coverage is excellent for most years. From 2008 to 2013, there are at least 346 nights with data per year, and the only major data gap was between March and July 2014 (see http://www.iafe.uba.ar/aeronomia/Months.html).

The SABER instrument measures height profiles of various atmospheric parameters, since late January 2002, including temperatures derived from the brightness of CO_2 emissions (see, e.g., Rezac et al., 2015 and references therein). Here we use nocturnal temperatures, in the height range of interest to us, from 2002 to 2014 (data version V2.0, see http://saber.gats-inc.com/temp_errors.php).

For better comparison with our AAS data, we calculate “airglow-equivalent” SABER temperatures, for which SABER temperature profiles are averaged with Gaussian weight functions. These weight functions are centered at 87 km (for OH) or 95 km (for O_2), with 8 km full width at half maximum (to represent the typical shape of both airglow layers). We have used the same parameters with CRISTA profiles (Scheer et al., 2006) and more recently also with SABER profiles (Scheer and Reisin, 2013). Similar approaches have been used by other investigators (e.g., for OH, French and Mulligan, 2010).

We always use an average over all SABER temperatures at tangent points inside a miss distance circle centered at LEO with 1000 km radius. To reduce the mean miss distance, only overpasses with at least 3 tangent points (TP) are taken into account (up to 6 TPs may occur), which leads to a mean miss distance of 370 km. In what follows, we always use the term “overpass” with these conditions implied.

We treat SABER data separately, according to whether the satellite is on the western (“*fromW*”) or eastern side (“*fromE*”) of the TP. Since such a distinction, to our knowledge, has not been made in the literature, the following explanations may be warranted. The satellite position with respect to the TP depends on the orbital node (ascending or descending), but not only. It also depends on the phase of the yaw cycle (“North viewing” or “South viewing” in the expression used by Russell III et al., 1999; see also Zhang et al., 2006 for a thorough discussion of these topics). The relation between orbital node and *fromE* or *fromW* observing perspective is inverted in each yaw maneuver, which the satellite performs after (approximately) 60 days, during the odd-numbered months (January, March, ..., November). More precisely, in the North viewing phase, SABER observes from West in the descending node (Fig. 1, left), but in the South viewing phase, in the ascending mode (Fig. 1, right). The opposite holds for observation from East. The North viewing phase of the yaw cycle is centered on February, June, and October, and the South viewing phase on April, August, and December. Since the distance between SABER and the TP is about 2600 km, the satellite position for *fromW* observations is well over the Pacific, and for *fromE* observations clearly in the South Atlantic Anomaly area.

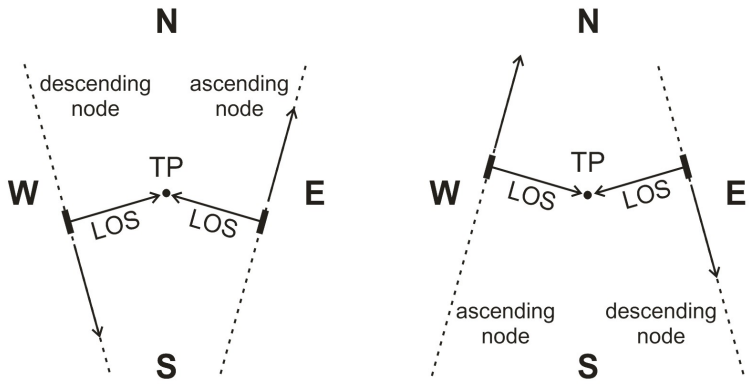

Fig. 1. Schematic maps of SABER observing geometry for the “North viewing” (left) and “South viewing” phase (right) of the satellite yaw cycle, showing the line of sight (LOS) from the satellite position to the tangent point (TP) for the ascending and descending orbital nodes.

3. Results

3.1. All LEO overpasses

First we consider the SABER data of all LEO overpasses, whether there are simultaneous AAS data or not. This means, for 2002 to 2014 all the overpasses (compliant with the selection criteria mentioned) are used, which includes the years practically without any AAS data (2003 to 2005). The annual averages of the nocturnal airglow-equivalent SABER temperatures around LEO are obtained separately for both perspectives (*fromE* and *fromW*). Temperatures *fromE* are systematically higher than temperatures *fromW* for all years and for both airglow-equivalent altitudes (Fig. 2). Each annual mean is based on no less than 179 overpasses (each containing 4.4 profiles, on average) leading to statistical errors smaller than 0.77 K. The differences between the OH-equivalent temperatures *fromE* and *fromW* vary between 2.36 K and 5.86 K. We will here refer to these differences always with the symbol ΔT, independently of how and in which context they are obtained. The ΔT of O_2-equivalent temperatures ranges from 2.31 K to 5.61 K (Table 1). Mean ΔT over all years is 4.45 (±0.23) K for OH, and 3.46 (±0.26) K for O_2. These values are considerable and need to be explained.

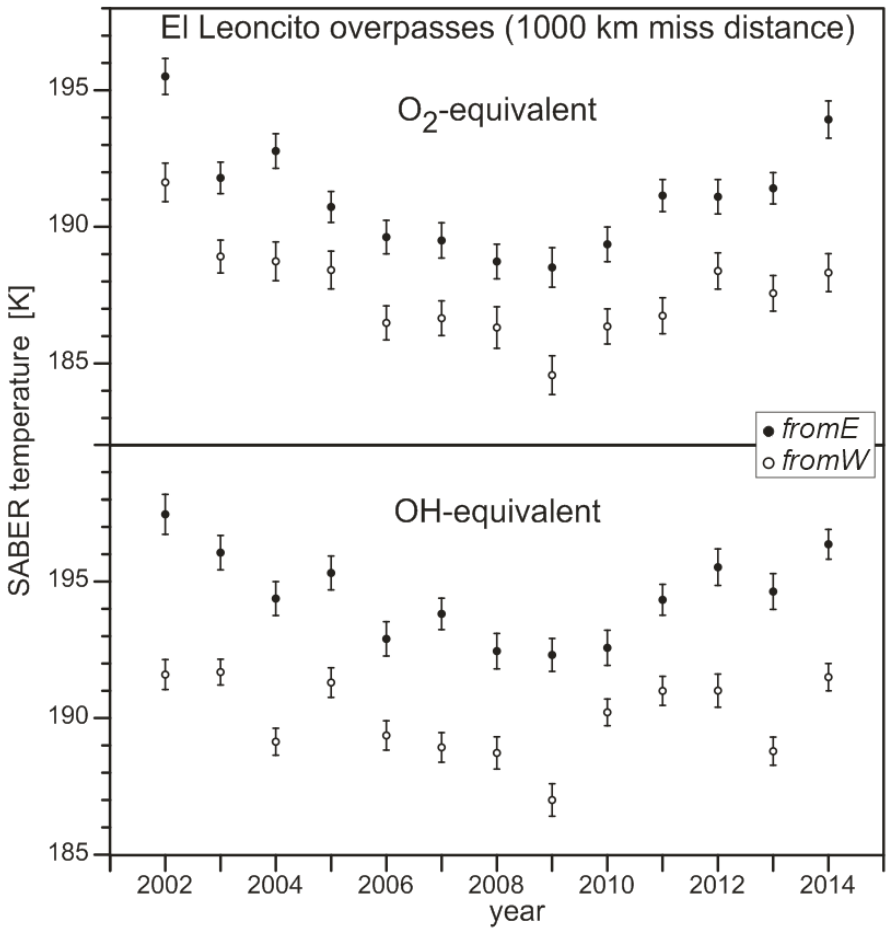

Fig. 2. Yearly averages of airglow-equivalent nocturnal temperatures measured by SABER over El Leoncito (LEO), separately for both observing perspectives (*fromE*, *fromW*).

Table 1
Annual number of SABER overpasses at LEO, and temperature differences ΔT between the two observing perspectives (*fromE*, *fromW*) at OH and O_2 airglow-equivalent heights.

	# fromE	*# fromW*	ΔT (OH) [K]	ΔT (O_2) [K]
2002	181	185	5.86 ± 0.92	3.88 ± 0.97
2003	200	189	4.37 ± 0.79	2.88 ± 0.83
2004	194	193	5.24 ± 0.79	4.04 ± 0.95
2005	194	198	4.01 ± 0.82	2.31 ± 0.89
2006	192	197	3.53 ± 0.83	3.14 ± 0.87
2007	194	190	4.89 ± 0.79	2.85 ± 0.91
2008	195	189	3.73 ± 0.88	2.42 ± 0.99
2009	183	179	5.31 ± 0.85	3.94 ± 1.01
2010	194	188	2.36 ± 0.81	3.01 ± 0.90
2011	197	194	3.33 ± 0.78	4.40 ± 0.88
2012	198	193	4.52 ± 0.90	2.72 ± 0.92
2013	210	194	5.84 ± 0.83	3.84 ± 0.87
2014	198	193	4.86 ± 0.74	5.61 ± 0.97
total	**2530**	**2482**	**4.45 ± 0.23**	**3.46 ± 0.26**

We will first show that the seasonal distribution of the number of overpasses *fromE* or *fromW* has very little impact on the observed ΔT. Since we are dealing only with nocturnal data, this distribution is not approximately constant, but rather complex, due to TIMED orbital drift and the periodic yaw maneuvers. This leads to a tendency of the measurements to alternate between *fromE* and *fromW* groups in different parts of the year, nearly in phase with the yaw cycle. The total number of overpasses from 2002 to 2014 versus season is often about 12 per day-of-year, but there are also spells of up to 18 nights without a single overpass (see Fig. 3). The seasonal variation of temperature, in combination with the temporal structure of the overpasses is completely insufficient to account for the observed ΔT values. To remove the seasonal variation from the SABER data, we use the local ground-based climatology by Reisin and Scheer (2009). This leads to a mean ΔT equal to 4.48 (±0.22) K for OH and 3.61 (±0.26) K and O_2, very nearly identical to the uncorrected values. This means that the effect of the seasonal temperature variation is indeed negligible.

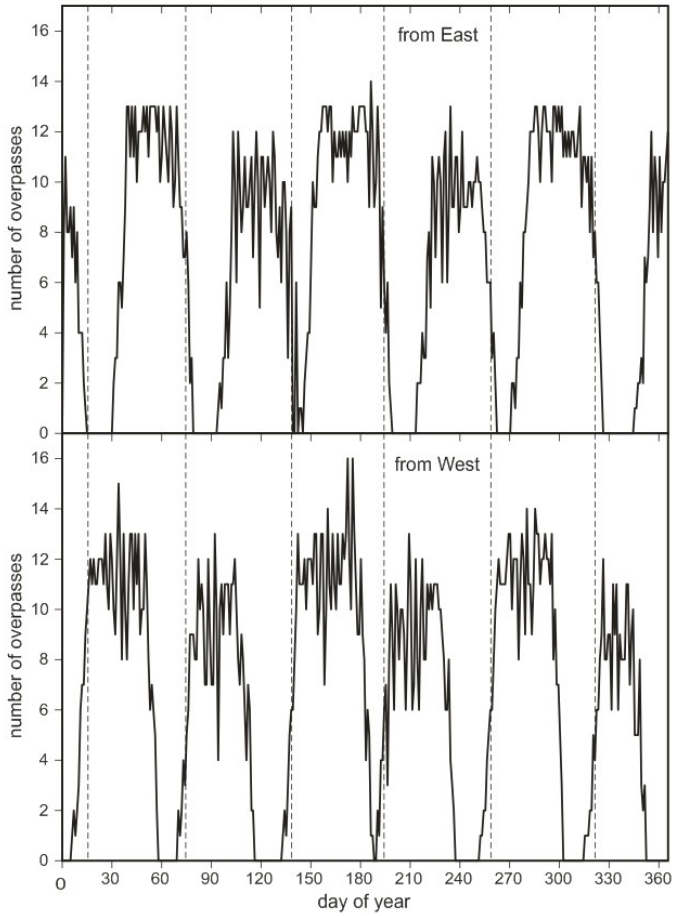

Fig. 3. Seasonal variation of the number of nocturnal SABER overpasses at LEO for both observing perspectives, and mean yaw maneuver dates (dashed lines).

The coverage of the tangent points within the 1000 km miss distance circle around LEO is sufficiently uniform so that there cannot be a major impact on ΔT. Only the latitudinal

distribution shows some surprising systematic bias. This bias consists in that some of the 11326 *fromW* TPs are somewhat more frequent towards higher latitudes than those *fromE* (see Fig. 4). With the 10830 *fromE* TPs, there is slightly greater abundance at low latitudes, in comparison with the *fromW* TPs. The mean over all *fromW* TPs corresponds to the geographical position 32.65ºS, 69.32ºW, while the mean *fromE* is at 31.63ºS, 69.23ºW (only 20 km from LEO). The latitudinal difference of only 1º between both mean positions is insufficient to explain the large values of ΔT.

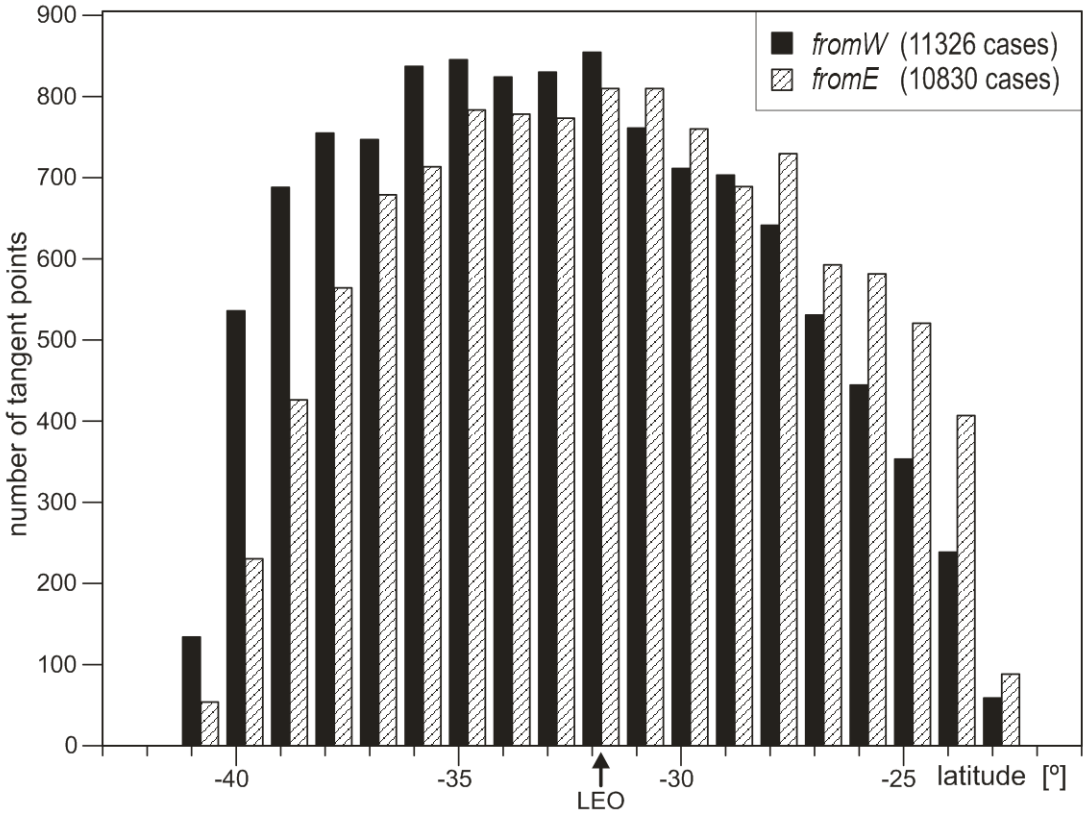

Fig. 4. Latitudinal distribution of the number of SABER tangent points within 1000 km of LEO, *fromE* (hatched) and *fromW* (black). Bin size is 1º, shifted into alignment with LEO latitude (at -31.8º).

We have also done an analysis of ΔT from SABER by changing the centroid height as if it were a free parameter, to see how emission height changes might affect observations. The results from 80 km to 102 km in one-kilometer steps form a smooth variation of ΔT with height, as shown in Fig. 5. The error bars grow slowly from 0.18 K at 80 km to 0.36 K at 102 km (they are so small because of the massive averaging involved). Of course, for the nominal airglow altitudes (marked by dashed lines), the values coincide with the total mean values given in Table 1. With respect to the observed variability of the OH emission of about ±1 km (e.g., Gao et al. 2010), Fig. 5 suggests changes in ΔT

of only about ±1 K. Around the nominal altitude of O_2, the size of the effect is similar, but with the opposite sign.

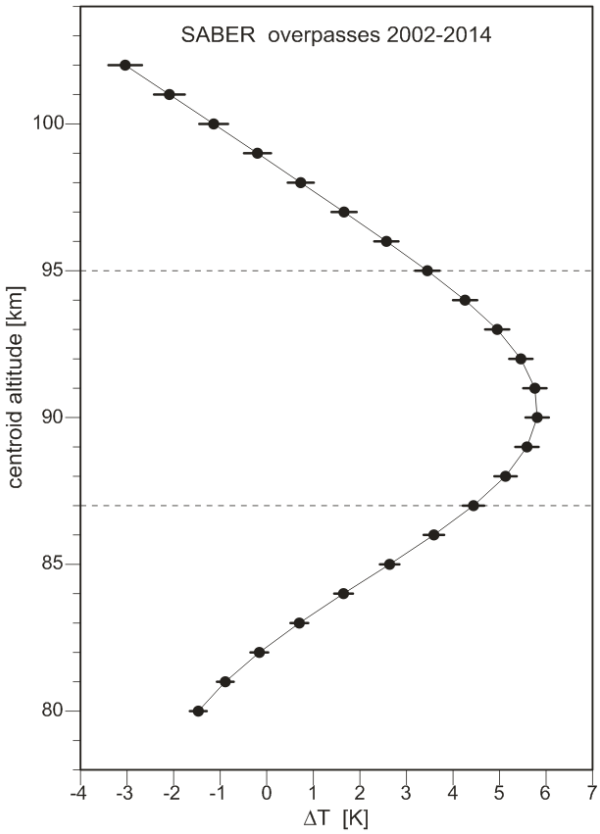

Fig. 5. Changes of Δ*T* under hypothetical variation of centroid emission altitude. Nominal OH and O_2 emission altitudes are marked by dashed lines.

3.2. Comparison of SABER with AAS results

We will now compare temperature differences Δ*T* derived from SABER and from ground-based measurements at LEO. Note that this does not involve a direct intercomparison of SABER and AAS temperatures (which has not been done for reasons described in Scheer and Reisin, 2013), because Δ*T* is independent of eventual systematic offsets between the respective temperature scales.

We will here only use the data from 2006 to 2014, and those overpasses that are accompanied by simultaneous data from AAS. To approach zero-miss time and reduce data variance, 30-minute averages of AAS temperatures centered on mean overpass time are used. Also, we only include cases with at least 15 data points and low noise. This results in 1093 *fromE* and 1003 *fromW* overpasses and the corresponding ground-based averages for OH. For O_2, these numbers are 899 and 697, respectively. Part of the differences may be due to the somewhat higher noise level of the ground-based O_2

temperatures (Scheer and Reisin, 1990), because the same upper noise limit as for OH was applied for O_2.

From this subset of overpasses, i.e. only those accompanied by ground-based data, new SABER temperature differences ΔT are determined, for each year. Note that the overall results of this subset, of 4.10 (±0.35) K for OH and 3.00 (±0.45) K for O_2, agree within error bars with the complete dataset of Table 1. The ground-based data are now also grouped according to the viewing perspective of the satellite instrument. One might argue that such a grouping does not really make sense for lack of any direct link between satellite position and AAS, but the results will show that it does. So, the AAS temperature differences between both data groups can be compared to the corresponding SABER results. For OH, the yearly ΔT values obtained with SABER and AAS agree very well (Fig. 6). Even for 2009 and 2014 the yearly averages differ by only one standard error of the mean. For O_2, differences are greater but still within combined error bars (with the exception of a major difference for 2007).

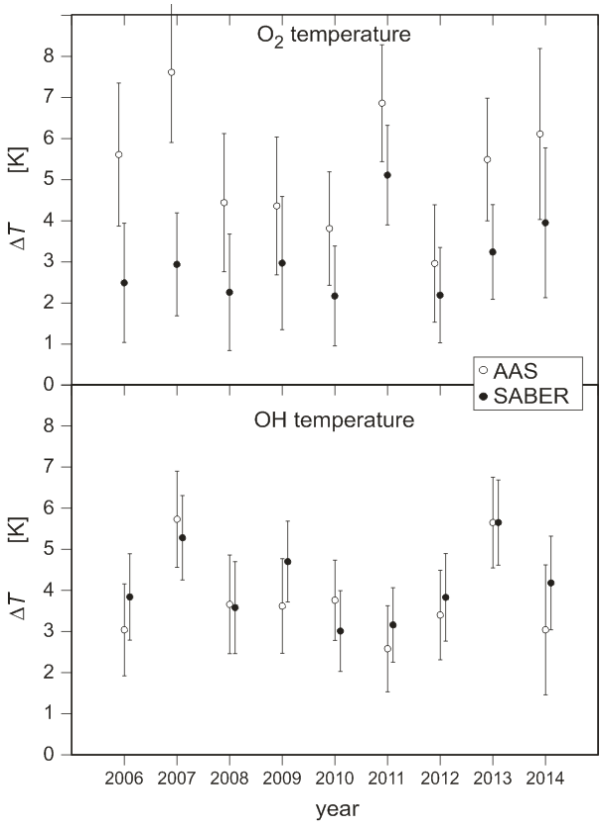

Fig. 6. Annual ΔT values (from SABER and AAS) for SABER overpasses at LEO (see text for details).

On average over all these years, ΔT values for OH are also in good agreement for both instruments, the difference being consistent with zero (Table 2). On the other hand, there is a significant difference for O_2 with ΔT about 2 K smaller for SABER than for AAS.

The reason for this is not clear. While Fig. 5 suggests that lowering the O_2 emission height to 92 km would remove the discrepancy, this does not seem to be a valid explanation, unless independent observations confirm such a low mean O_2 emission height.

Table 2
Total averages of ΔT for SABER overpasses at LEO simultaneous with AAS measurements, ΔT for AAS data, and differences between SABER and AAS.

	ΔT (OH) [K]	ΔT (O_2) [K]
SABER	4.10 ± 0.35	3.00 ± 0.45
AAS	3.83 ± 0.38	5.13 ± 0.55
SABER-AAS	0.27 ± 0.52	-2.13 ± 0.71

The main message is that AAS measurements give ΔT values that are similar (or even greater) than those from SABER. This means that we can discard an artifact due to the satellite position, like possible responses to precipitating particles in the South Atlantic Anomaly area (see, e.g., Štěpánek et al., 2013, for maps of the geographical distribution of DORIS oscillator drift). Rather, the observed effect must be related to the temporal distribution of data samples.

3.3. Monthly distribution

For a more detailed look at the temporal distribution, we compute ΔT for each month averaged over the years 2006 to 2014, separately for SABER and AAS. While there is considerable variability from month to month, data for SABER and AAS agree more often than not, even when only counting agreements within a single error bar. The same holds for OH and O_2 (see Fig. 7; but note that the ΔT scale is about four times greater than in Fig. 6).

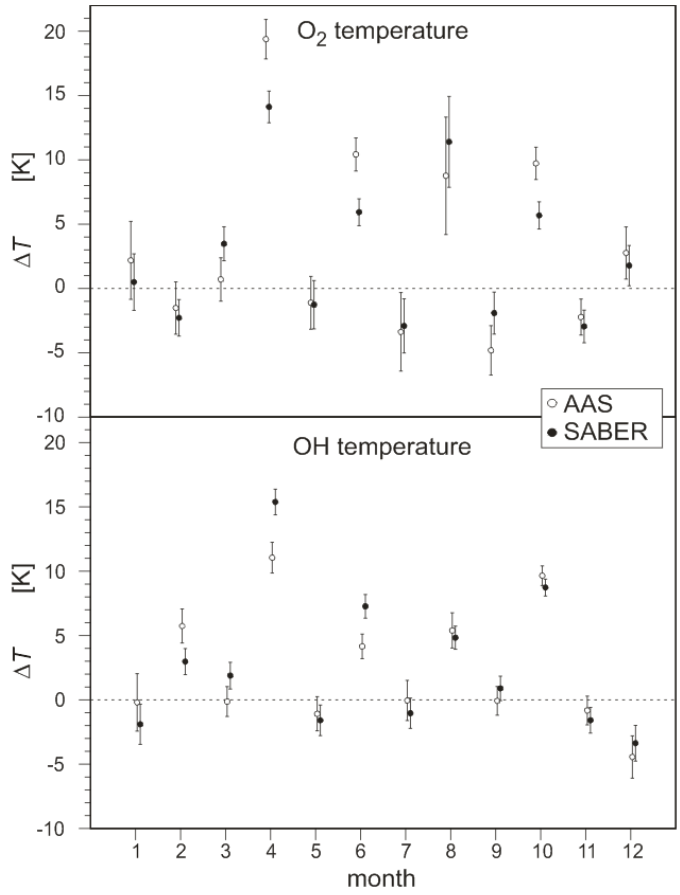

Fig. 7. Monthly Δ*T* values (from SABER and AAS) for SABER overpasses at LEO.

For OH, Δ*T* values close to zero correspond to the odd-numbered months. For O_2, these months have also low, or even slightly negative, Δ*T* values. This means that these months essentially do not contribute to the net effect of the total Δ*T*. On the other hand, some months have high Δ*T* values (for OH and O_2), especially April, but also June, August and October, which are thus the main contributors to the total Δ*T*.

3.4. Local time distribution

As mentioned, the local time distribution of the data is important for understanding the observed effects. We now consider the local time distribution of SABER overpasses for each month, separately for *fromE* and *fromW* measurements, again for overpasses with simultaneous AAS data. The local time distributions vary because of the orbital precession of the satellite and the periodic yaw maneuvers.

There are great differences between the distributions for odd-numbered and even-numbered months. The distributions *fromE* and *fromW* overlap for the odd-numbered months (see Fig. 8). Note that this is not a consequence of the yaw maneuvers which

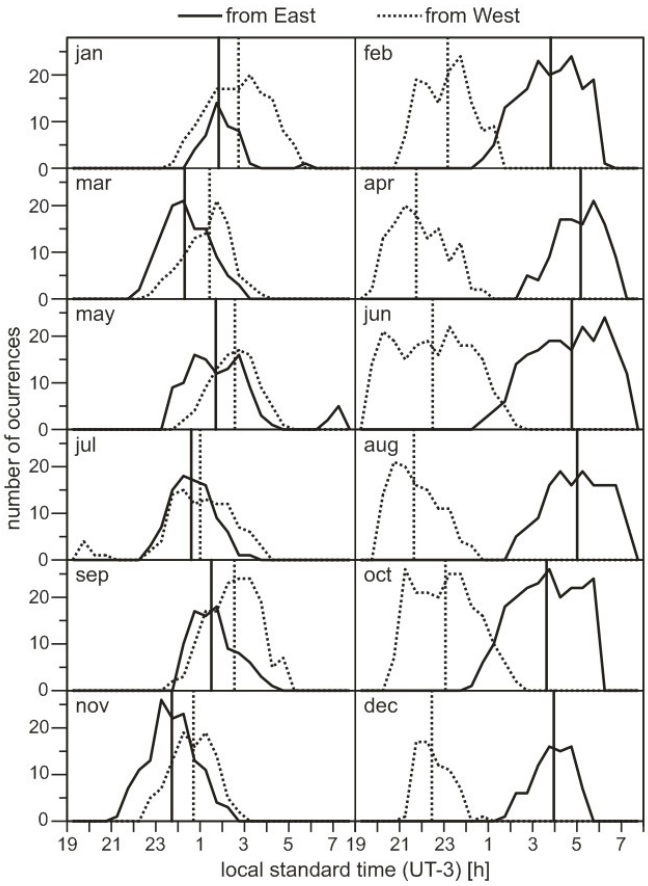

Fig. 8. Hourly distributions of the number of SABER overpasses at LEO for each month (30 minute bins), *fromE* (solid) and *fromW*(dotted), and the corresponding medians (vertical lines).

occur in these months, but the yaw maneuvers do cause the coexistence of both distributions in the same months. On the other hand, there is little or no overlap for the even-numbered months, where the overpasses *fromW* occur considerably earlier than those *fromE*. These differences can be described more easily by comparing the medians of the distributions. For the odd-numbered months, the medians *fromE* occur about one hour **before** the medians *fromW* (24 minutes earlier, for July). For the other months, the medians *fromE* occur between 4.5 and 7.5 hours **later** than the medians *fromW*. The relevance of these distributions in the present context is that they define the moments when the mean nocturnal variations at LEO are sampled by AAS, and by SABER.

3.5. Monthly mean tides at LEO

The AAS temperature data set from 2006 to 2014 serves to establish the mean nocturnal variation for each month. Each monthly mean is thus solidly based on at least 220 individual nights (with an average of 247), although not all nights are documented completely (but mean nocturnal coverage is 7 hours). The most salient feature is the strong semidiurnal tidal variation in all six months from April to September (see Fig. 9).

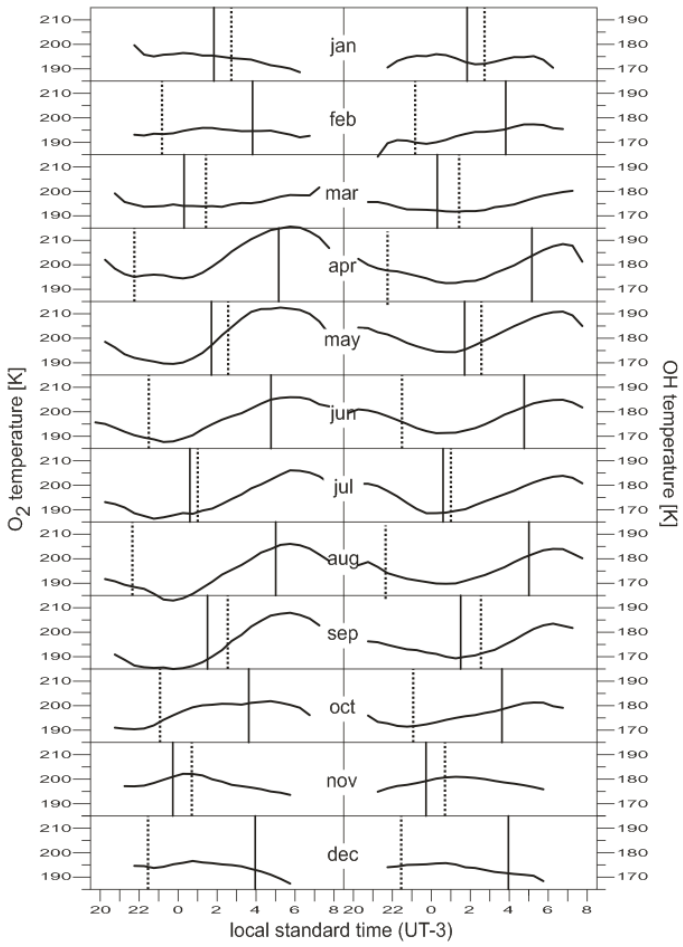

Fig. 9. Monthly mean nocturnal variations of O_2 temperature (left) and OH temperature (right), from AAS data for 2006 to 2014, and medians of the hourly overpasses (vertical lines from Fig. 8; solid: *fromE*, dotted: *fromW*).

For these months, the main spectral component has amplitudes from 6.3K to 7.5K for OH and from 8.7K to 12.1K for O_2. The tidal origen of the semidiurnal variations, otherwise difficult to ascertain from measurements at a single site, becomes plausible because of the nearly constant phase, from month to month. This phase, expressed as the time when the sinusoid assumes its maximum, varies only between 6.4 and 7.4 hours (LST) for OH and between 5.2 and 6.3 hours for O_2 (see Table 3). The phase of the O_2 oscillation is advanced by 0.5 to 1.6 hours with respect to the OH oscillation, consistent with upward energy propagation (these phases are evaluated at the center of each time interval, which is necessary when periods are somewhat different, as in June, July, and October). In October, the tidal amplitudes are weaker and phases are earlier. The phase shift is still consistent with upward energy propagation, only slightly greater than in the six previous months. In the five months from November to March, there are no clear tidal signatures (therefore these months are not included in Table 3).

Table 3
Period (P), amplitude (A), and phase (ϕ = time of maximum) of the main spectral component of monthly mean nocturnal variation for OH and O_2 temperature, and phase difference between OH and O_2 ($\Delta\phi$; see text for how this is defined).

month	P(OH) [h]	A(OH) [K]	ϕ(OH) [h]	P(O_2) [h]	A(O_2) [K]	ϕ(O_2) [h]	$\Delta\phi$ [h]
APR	12.7	6.8	7.0	12.9	10.6	5.6	1.4
MAY	11.8	7.5	6.4	12.1	12.1	5.2	1.2
JUN	11.7	6.3	6.4	13.4	8.7	5.8	0.9
JUL	11.4	7.2	6.5	13.9	9.1	6.3	0.5
AUG	12.3	6.7	6.5	12.7	10.6	5.7	0.9
SEP	13.5	6.7	7.4	12.9	11.6	5.8	1.6
OCT	12.4	4.3	5.3	14.9	6.1	3.6	2.0

Although not inmediately relevant here, it may be worthwhile to point out that previous unpublished monthly mean nocturnal temperature (and also intensity) variations measured by AAS (at the same site) between August 1997 and July 2000 already showed a similarly strong tidal variation in the same months as now (see the figure at http://www.iafe.uba.ar/aeronomia/monmean.gif). This strengthens the climatological interpretation of our present findings.

To appreciate the effect of the different sampling times of *fromE* and *fromW* measurements on ΔT, the medians of the overpass time distributions (from Fig. 8) can be taken into account as approximate sampling times of the monthly mean variation. This means that, in April, June, August and October and similarly for OH and O_2, the median of the *fromW* measurements sample the tide at low temperature while measurements *fromE* sample at high temperature (Fig. 9). This is, at least qualitatively, consistent with the strong positive values of monthly ΔT. For the remaining months, the effect on ΔT is small, either because measurement samples are not far apart (in the odd-numbered months, see Fig. 8) or because nocturnal variations are small (in February and December, see Fig. 9). Such a crude analysis already distinguishes clearly between the months that do contribute and those that do not contribute appreciably to the observed effect.

The analysis can be improved by taking the local time distributions of the overpasses, rather than the corresponding medians, into account. This is done by convoluting the monthly mean nocturnal variations with the overpass distributions, separately for both observation perspectives (*fromE* and *fromW*), so that independent values of ΔT can be obtained. The results are shown in Fig. 10, in comparison to the monthly mean ΔT

values obtained with AAS (same as Fig. 7). There is good agreement within one error bar, for almost all months. We can therefore reasonably attribute the observed perspective effect to the monthly mean nocturnal variation, mostly due to the semidiurnal tide. The satellite position with respect to the tangent point matters only because of its indirect impact on the local time distribution of the SABER overpasses.

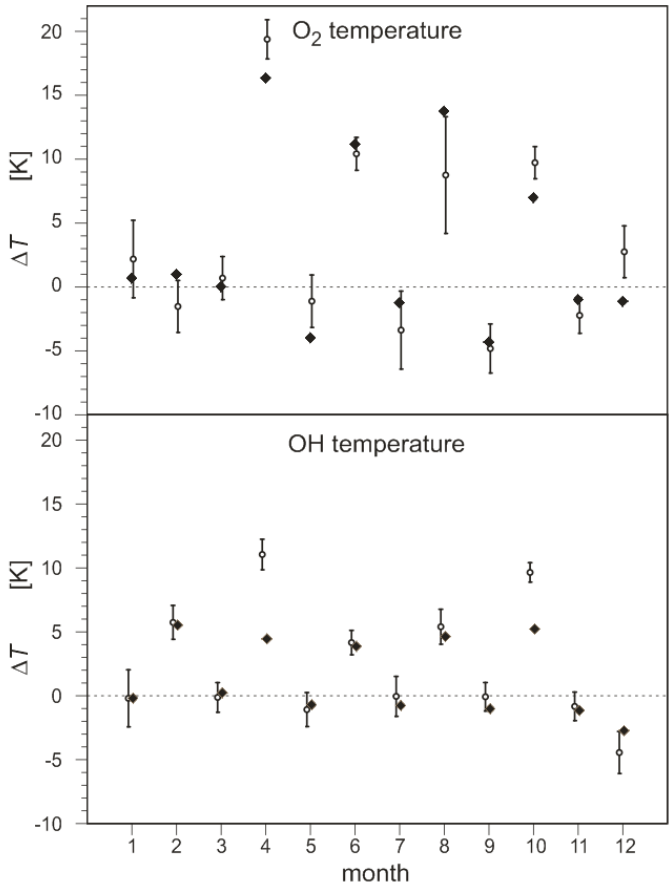

Fig. 10. Monthly Δ*T* values derived from the convolution between hourly overpass distribution and averaged nocturnal variation (black squares) in comparison with original AAS results (circles with error bars; same as in Fig. 7).

4. Conclusions

In this paper, we have used ground-based rotational temperatures from OH and O_2 airglow at El Leoncito (LEO) as well as airglow-equivalent SABER temperatures for LEO overpasses.

For all the SABER temperatures from 2002 to 2014, there are considerable systematic differences depending on the satellite position. When SABER looks towards LEO from the Atlantic Ocean, temperatures are higher than when viewed from the Pacific, which is unexpected. The difference is 4.45 (±0.23) K for OH-equivalent and 3.46 (±0.26) K for O_2-equivalent heights, and appears at first sight to be an effect of the satellite position.

The simultaneous ground-based measurements (from 2006 to 2014), when separately processed according to the satellite position, reproduce this satellite perspective effect. This surprising finding implies that a direct relation to satellite position can be ruled out, and therefore, also excludes the possibility of an appreciable SABER artifact due to the South Atlantic Anomaly.

Our monthly analysis shows that the total perspective effect is mainly due to the contributions of data from April, June, August and October. The monthly local time distributions of the overpasses for both satellite perspectives differ strongly between odd- and even-numbered months. On the other hand, the ground-based instrument supplies sufficient data to define a climatology of monthly means for the nocturnal temperature variation. This climatology shows a strong semidiurnal tide from April to September reaching amplitudes of 7.5 K for OH and 12 K for O_2.

The perspective effect can therefore be understood as a consequence of the local time sampling (defined by the satellite) and the mean nocturnal temperature variation (observed by the ground-based instrument). That is, the convolution of the monthly nocturnal variations with the local time distributions of overpasses leads to results consistent with the observed ground-based and satellite-based perspective effects. The main contributions are from those even-numbered months when the semidiurnal tide is strong, while the odd-numbered months only make small contributions because of the similar overpass timing for both perspectives.

A general “lesson learned” is that comparison of SABER temperatures with ground-based data at any site inevitably involves the details of the overpass time structure and nocturnal variations. The nocturnal variations are expected to be dominated by the tides, and not only by the semidiurnal tide, as in the present case. Therefore, perspective effects at other sites can be expected to depend on latitude, and maybe even on longitude. Even if there is a balance between the number of cases with the two observation perspectives, mean temperatures may still have some bias.

This issue may even have consequences outside the context of intercomparison between SABER and ground-based temperatures. Global maps based only on SABER temperatures may also be somewhat affected, unless corrections for the local tide are applied. Ground-based measurements should be helpful to produce such corrections.

Although the results presented here apply strictly only to SABER temperatures, other instruments on the same or on different satellites may, of course, produce analogous (though probably different) sampling time effects.

Acknowledgements: The authors thank the staff of *Complejo Astronómico El Leoncito* (CASLEO) for continuous support during the AAS measurements, and also to the SABER team for permitting access to the SABER data via the http://saber.gats-inc.com/ web site. Partial funding by CONICET under D3646 (02-10-2014) - 45259 is also gratefully acknowledged. We thank the three anonymous reviewers for helpful comments.

References

French, W.J.R., Mulligan, F.J., 2010. Stability of temperatures from TIMED/SABER v1.07 (2002-2009) and Aura/MLS v2.2 (2004-2009) compared with OH(6-2) temperatures observed at Davis Station, Antarctica. Atmos. Chem. Phys., 10, 11439-11446.

Gao, H., Xu, J., Wu, Q., 2010. Seasonal and QBO variations in the OH nightglow emission observed by TIMED/SABER. J. Geophys. Res., 115, A06313, doi:10.1029/2009JA014641.

Kumar, K.K., Vineeth, C., Antonita, T.M., Pant, T.K., Sridharan, R., 2008. Determination of day-time OH emission heights using simultaneous meteor radar, day-glow photometer and TIMED/SABER observations over Thumba (8.5°N, 77°E). Geophys. Res. Lett., 35(18), L18809, doi:10.1029/2008GL035376.

Liu, W., Xu, J., Smith, A.K., Yuan, W., 2015. Comparison of rotational temperature derived from ground-based OH airglow observations with TIMED/SABER to evaluate the Einstein coefficients. J. Geophys. Res., 120, 10069-10082, doi:10.1002/2015JA021886.

López-González, M.J., García-Comas, M., Rodríguez, E., López-Puertas, M., Shepherd, M.G., Shepherd, G.G., Sargoytchev, S., Aushev, V.M., Smith, S.M., Mlynczak, M.G., Russell, J.M., Brown, S., Cho, Y.-M., Wiens, R.H., 2007. Ground-based mesospheric temperatures at mid-latitude derived from O_2 and OH airglow SATI data: Comparison with SABER measurements. J. Atmos. Sol.-Terr. Phys., 69(17-18), 2379-2390.

Mulligan, F.J., Lowe, R.P., 2008. OH-equivalent temperatures derived from ACE-FTS and SABER temperature profiles - a comparison with OH*(3-1) temperatures from Maynooth (53.2°N, 6.4°W). Ann. Geophys., 26, 795-811.

Niciejewski, R., Wu, Q., Skinner, W., Gell, D., Cooper, M., Marshall, A., Killeen, T., Solomon, S., Ortland, D., 2006. TIMED Doppler Interferometer on the Thermosphere Ionosphere Mesosphere Energetics and Dynamics satellite: Data product overview. J. Geophys. Res., 111(A11), A11S90, doi:10.1029/2005JA011513.

Oberheide, J., Offermann, D., Russel III, J.M., Mlynczak, M.G., 2006. Intercomparison of kinetic temperatures from 15 μm CO_2 limb emissions and OH*(3,1) rotational temperature in nearly coincident air masses: SABER, GRIPS. Geophys. Res. Lett., 33, L14811, doi:10.1029/2006GL026439.

Reisin, E.R., Scheer, J. 2009. Evidence of change after 2001 in the seasonal behaviour of the mesopause region from airglow data at El Leoncito. Adv. Space Res., 44(3), 401-412.

Reisin, E.R., Scheer, J., Dyrland, M.E., Sigernes, F., Deehr, C.S., Schmidt, C., Höppner, K., Bittner, M., Ammosov, P.P., Gavrilyeva, G.A., Stegman, J., Perminov, V.I., Semenov, A.I., Knieling, P., Koppmann, R., Shiokawa, K., Lowe, R.P., López-González, M.J., Rodríguez, E., Zhao, Y., Taylor, M.J., Buriti, R.A., Espy, P.J., French, W.J.R., Eichmann, K.U., Burrows, J.P., von Savigny, C., 2014. Traveling planetary wave activity from mesopause region airglow temperatures determined by the Network for the Detection of Mesospheric Change (NDMC). J. Atmos. Sol.-Terr. Phys., 119, 71-82, doi:10.1016/j.jastp.2014.07.002.

Remsberg, E.E., Marshall, B.T., Garcia-Comas, M., Krueger, D., Lingenfelser, G.S., Martin-Torres, J., Mlynczak, M.G., Russell, J.M., Smith, A.K., Zhao, Y., Brown, C., Gordley, L.L., Lopez-Gonzalez, M.J., Lopez-Puertas, M., She, C.-Y., Taylor, M.J., Thompson, R.E., 2008. Assessment of the quality of the Version 1.07 temperature-versus-pressure profiles of the middle atmosphere from TIMED/SABER. J. Geophys. Res., 113(D17), D17101, doi:10.1029/2008JD010013.

Rezac, L., Kutepov, A., Russell III, J.M., Feofilov, A.G., Yue, J., Goldberg, R.A., 2015. Simultaneous retrieval of T(p) and CO_2 VMR from two-channel non-LTE limb radiances and application to daytime SABER/TIMED measurements. J. Atmos. Sol.-Terr. Phys., 130-131, 23-42.

Russell III, J.M., Mlynczak, M.G., Gordley, L.L., Tansock, J., Esplin, R., 1999. An overview of the SABER experiment and preliminary calibration results. Proc. SPIE, 3756, 277-288.

Scheer, J., 1987. Programmable tilting filter spectrometer for studying gravity waves in the upper atmosphere. Appl. Opt., 26, 3077-3082.

Scheer, J., Reisin, E.R., 1990. Rotational temperatures for OH and O_2 airglow bands measured simultaneously from El Leoncito (31°48'S). J. Atmos. Terr. Phys., 52, 47-57.

Scheer, J., Reisin, E.R., 2001. Refinements of a classical technique of airglow spectroscopy. Adv. Space Res., 27(6-7), 1153-1158.

Scheer, J., Reisin, E.R., 2013. Simpson's paradox in trend analysis: An example from El Leoncito airglow data. J. Geophys. Res., 118, 5223-5229, doi:10.1002/jgra.50461.

Scheer, J., Reisin, E.R., Gusev, O.A., French, W.J.R., Hernandez, G., Huppi, R., Ammosov, P., Gavrilyeva, G.A., Offermann, D., 2006. Use of CRISTA mesopause region temperatures for the intercalibration of ground-based instruments. J. Atmos. Sol.-Terr. Phys., 68(15),doi:10.1016/j.jastp.2005.12.009, 1698-1708.

Siskind, D.E., Coy, L., Espy, P., 2005. Observations of stratospheric warmings and mesospheric coolings by the TIMED SABER instrument. Geophys. Res. Lett., 32(9), L09804, doi:10.1029/2005GL022399.

Smith, S.M., Baumgardner, J., Mertens, C.J., Russell, J.M., Mlynczak, M.G., Mendillo, M., 2010. Mesospheric OH temperatures: Simultaneous ground-based and SABER OH measurements over Millstone Hill. Adv. Space Res., 45, 239-246.

Štěpánek, P., Douša, J., Filler, V., 2013. SPOT-5 DORIS oscillator instability due to South Atlantic Anomaly: mapping the effect and application of data corrective model. Adv. Space Res., 52(7), 1355-1365.

von Savigny, C., Eichmann, K.-U., Llewellyn, E.J., Bovensmann, H., Burrows, J.P., Bittner, M., Höppner, K., Offermann, D., Taylor, M.J., Zhao, Y., Steinbrecht, W., Winkler, P., 2004. First near-global retrievals of OH rotational temperatures from satellite-based Meinel band emission measurements. Geophys. Res. Lett., 31, L15111, doi:10.1029/2004GL020410.

Xu, J., She, C.Y., Yuan, W., Mertens, C., Mlynczak, M., and Russell, J., 2006. Comparison between the temperature measurements by TIMED/SABER and lidar in the midlatitude. J. Geophys. Res., 111(A10), A10S09, doi:10.1029/2005JA011439.

Yuan, T., She, C.-Y., Krueger, D., Reising, S., Zhang, X., Forbes, J.M., 2010. A collaborative study on temperature diurnal tide in the midlatitude mesopause region (41°N, 105°W) with Na lidar and TIMED/SABER observations. J. Atmos. Sol.-Terr. Phys., 72(5-6), 541-549.

Zhang, X., Forbes, J.M., Hagan, M.E., Russell III, J.M., Palo, S.E., Mertens, C.J., Mlynczak, M.G., 2006. Monthly tidal temperatures 20-120 km from TIMED/SABER. J. Geophys. Res., 111(A10), A10S08, doi:10.1029/2005JA011504.